Available online at www.scholarsresearchlibrary.com

Scholars Research Library

Der Pharmacia Lettre, 2016, 8 (5):260-273
(http://scholarsresearchlibrary.com/archive.html)

ISSN 0975-5071
USA CODEN: DPLEB4

Structural, Thermal and BSA binding analysis of L-Tryptophan derived Mn(III)/Fe(III) complexes

R. Biju Bennie[1], C. Joel[1], S. Daniel Abraham[1], S. Theodore David[1*] and S. Iyyam Pillai[2]

[1]P.G. Department of Chemistry, St. John's College, Tirunelveli-627002, Tamilnadu, India
[2]P.G. and Research Department of Chemistry, Pachaiyappa's College, Chennai-600030, Tamilnadu, India

---

ABSTRACT

A novel N_2O_2 type ligand has been synthesized from 9, 10- Phenanthrenequinone and L-tryptophan and complexed with Mn(III) and Fe(III) metal ions. The synthesized ligand and its complexes were characterized by various spectral techniques such as FT-IR, UV-visible, ^{13}C NMR, EPR, EI-Mass, elemental analysis, magnetic susceptibility and molar conductivity measurements. The metal complexes exhibit octahedral geometry. The thermal studies of the complexes were also carried out. The interaction of these synthesized metal complexes with Bovine Serum Albumin (BSA) has been studied using emission and absorption techniques. The Stern-Volmer quenching constants (K_{sv}), number of binding sites (n) and binding energy are calculated. It has been found that the metal complexes could bind to the hydrophobic pocket of BSA in sub-domain IIA. The energy transfer between the BSA and complexes have been studied using FRET and the donor acceptor distance was found to be less than 8 nm. The interaction of these metal complexes with BSA has been further supported by molecular docking studies.

Keywords: 9, 10- Phenanthrenequinone, L-tryptophan, BSA, FRET, molecular docking.

INTRODUCTION

Coordination chemistry plays a vital role in scores of biological reactions. Many ligands have been designed to mimic the function of natural carriers recognizing and transporting specific metal ions, anions or neutral molecules and in understanding and reproducing the catalytic activity of metallo-enzymes and proteins [1].

Proteins are the most abundant macromolecules in cells and are crucial in maintaining normal cell functions. Bovine serum albumin (BSA), one of the major components in plasma protein, plays an important role in transporting and metabolizing of many endogenous and exogenous compounds in metabolism. In this work, BSA was chosen as a target protein molecule for studying the interaction, because of its medical significance, unusual ligand-binding properties, availability, and structural homology with human serum albumin (HSA) [2].

Serum albumin has been one of the most extensively studied proteins for many years. It is the most abundant protein in blood plasma with a typical concentration of 50 g/L and functions as a transport protein for numerous endogenous and exogenous substances. It also plays an important role in regulating the colloid osmotic pressure of blood. It provides about 80% of the osmotic pressure and is responsible for the pH maintenance in blood. The serum albumin is a versatile protein, principally characterized by its remarkable ability of binding a wide range of insoluble endogenous and exogenous compound. Since the serum albumin was considered to be nonantigenic and biodegradable, and was readily available, the albumin has been used as a bio-material, such as drug delivery and novel hydrophilic carriers.

Binding of metal complexes with the most abundant carrier proteins (serum albumins) have also been a subject of interest as such drug-protein binding greatly influences absorption, drug transport, storage, metabolism and excretion properties of typical drugs in vertebrates [3].

The most outstanding property of albumins is their ability to bind reversibly a large variety of ligands [4]. Reagents that react with protein chains are extremely useful in chemistry and biology [5, 6]. BSA is made up of three linearly arranged, structurally homologous domains (I-III) and each domain in turn is the product of two sub-domains (A, B). It has two tryptophan residues that possess intrinsic fluorescence: Trp-134, which is located on the surface of sub-domain IB, and trp-212, locating within the hydrophobic binding pocket of sub-domain IIA [7]. Therefore fluorescence technique can be considered as a feasible method for the measurements. Because of its high sensitivity, rapidity and simpleness [8], fluorescence technique has been widely used drug-protein studies [9-11]. In silico, molecular docking simulations predict the binding sites on BSA.

Although studies have been performed on the interaction of metal complexes [12] and metal ions [13-17], with albumins, there is a lack of information about the interaction of amino acid complexes and albumin. Hence, we report the interaction of Mn(III) and Fe(III) complexes of tryptophan based ligand with Bovine Serum Albumin using emission, absorption and docking studies.

MATERIALS AND METHODS

The chemicals involved in this work were of AnalaR grade and the solvents used were of 99% purity. The ligands employed in our present investigation, viz. 9,10-Phenanthrenequinone (Aldrich) and L-tryptophan (Loba Chemie) were purchased in pure form and used as such. Bovine Serum Albumin (BSA) was purchased from Sigma and Tris Buffer was purchased from HI MEDIA.

The elemental analysis (C, H and N) data were analyzed using Carlo Erba 1108 model elemental analyzer. The ^{13}C NMR spectrum was recorded on a Bruker Advance DRX 300 FT-NMR spectrometer in $CDCl_3$ solution using TMS as standard. EI mass spectrum was recorded on a JEOL DX-303 EI mass spectrometer. FT-IR spectra of the synthesized ligand and its complexes were recorded on a JASCO FT IR / 4100 Spectrometer, in the wave number region of 4000-400 cm^{-1}. The electronic spectra of the complexes were computed in 200-800 nm wavelength range on a Perkin Elmer Lambda 35 spectrophotometer using DMSO as the solvent. Magnetic susceptibility measurements were computed on a modified Hertz SG8-5HJ model Gouy magnetic balance using $CuSO_4.5H_2O$ as the calibrant. Molar conductivity of the complexes was measured by using a Elico model SX 80 conductivity-bridge in DMSO as solvent. EPR spectrum was recorded at liquid nitrogen temperature using a JEOL TES 100 EPR spectrometer by means of DPPH as the g-marker. TG/DTG analysis of the complexes was performed on SIINT 6300 instrument in air.

2.1 Synthesis of ligand (L)

About 10 mmol of 9,10-Phenanthrenequinone (2.08 g) was taken in a two-neck flat bottomed flask containing 40 ml of ethanol. To this, 20 mmol of L-Tryptophan (4.08 g) dissolved in 20 mmol of sodium hydroxide was added. The reaction mixture was stirred for 10 hours to give a bright yellow colored precipitate. The precipitate was repeatedly washed with water and diethyl ether. It was then dried *in vacuum* over anhydrous calcium chloride. (Scheme 1) The product obtained was characterized by IR, EI-MS and ^{13}C-NMR spectroscopy.

Yield: 65%, m.p: 198 ^0C, Anal. Found.(%): C, 74.39; H, 4.79; N, 9.57; Calc.: C, 74.4; H, 4.8; N, 9.6; EI-MS: m/z, 580.21; IR (KBr, cm^{-1}): $\nu_{(C=N)}$, 1673 cm^{-1}, $\nu_{asy(COO-)}$, 1590 cm^{-1}, $\nu_{sy(COO-)}$, 1447 cm^{-1}, $\nu_{indole(-NH)}$, 3460; ^{13}C NMR (δ, ppm in $CDCl_3$) 163.68 (C=N), 180.44 (COO^-)

2.2 Synthesis of metal complexes

Finely powdered ligand (1 mmol; 0.58 g) is dissolved in 20 ml ethanol. To this, 20 ml ethanolic solution of 1 mmol metal salts (manganese(III) acetate-0.27 g and iron(III) chloride- 0.40 g) were added drop wise. Then the mixture was stirred and refluxed at 50 ^0C for 12 hours. The resulting solution was then slowly evaporated at room temperature and the product obtained was washed several times with ethanol and dried *in vacuo* over anhydrous calcium chloride. (Scheme 1)

MnL: Yield: 50%; Brown colour; Anal. Found.(%): C, 64.58; H, 4.47; N, 8.33 and Mn, 8.72; Calc.: C, 64.6; H, 4.5; N, 8.4; IR (KBr, cm^{-1}): $\nu_{(C=N)}$, 1659 cm^{-1}, $\nu_{asy(COO-)}$, 1583 cm^{-1}, $\nu_{sy(COO-)}$, 1439 cm^{-1}; $\nu_{(M-O)}$, 530; $\nu_{(M-N)}$, 430; Λ_m ($Smol^{-1}cm^2$) 51.35; μ_{eff} (BM) 4.94; UV-Vis. in DMSO, nm (transition): 300 (LMCT), 580 and 730 (d-d).

FeL: Yield: 68%; Green colour; Anal. Found.(%): C, 64.41; H, 4.46; N, 8.24 and Fe, 8.74; Calc.: C, 64.5; H, 4.5; N, 8.3; IR (KBr, cm^{-1}): $\nu_{(C=N)}$, 1663 cm^{-1}, $\nu_{asy(COO-)}$, 1576 cm^{-1}, $\nu_{sy(COO-)}$, 1402 cm^{-1}; $\nu_{(M-O)}$, 531; $\nu_{(M-N)}$, 439; Λ_m ($Smol^{-1}cm^2$) 51.95; μ_{eff} (BM) 5.76; UV-Vis. in DMSO, nm (transition): 300 (LMCT), 700 (d-d).

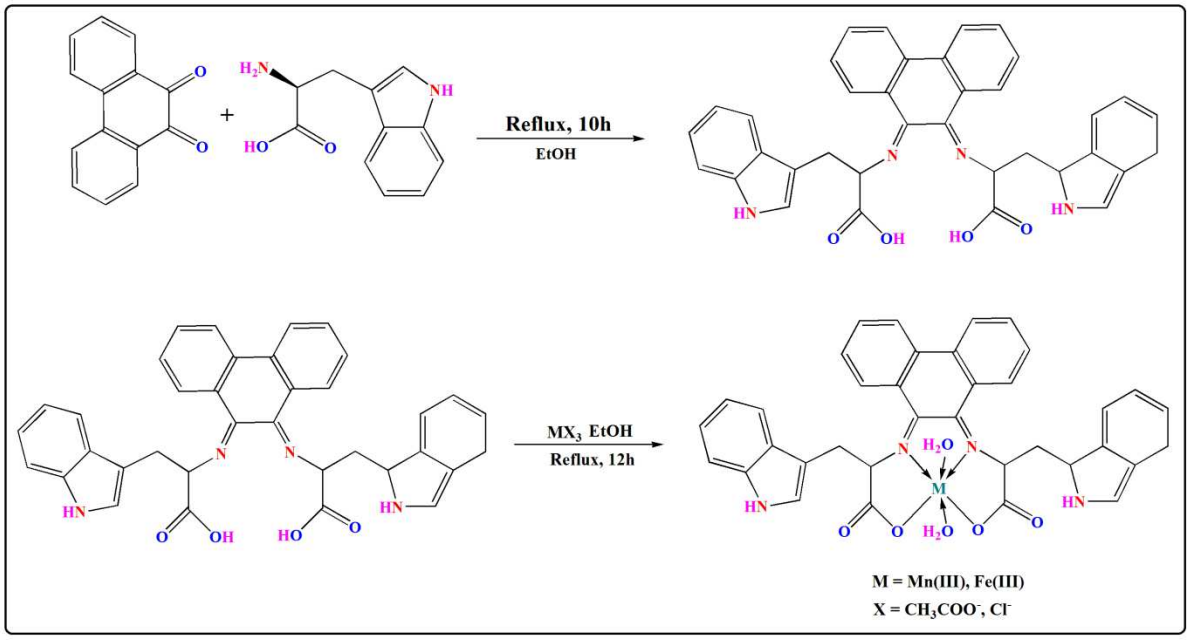

Scheme 1: Synthesis of the ligand (L) and its metal complexes (ML)

2.3 BSA binding experiments

2.3.1 Preparation of stock solutions

The concentrations of the stock solutions of BSA (C_{BSA} ~ 2 x 10^{-6} $molL^{-1}$) in tris buffer (0.05 $molL^{-1}$ Tris, 0.15 $molL^{-1}$ NaCl and the pH is maintained at 7.4 using con.HCl) are determined from absorption spectroscopy. The concentration is calculated by dividing absorbance at 280 nm by molar extinction coefficients of BSA (ε_{280} = 44,300 $M^{-1}cm^{-1}$) [18]. The stock solutions of metal complexes were prepared by dissolving them in DMF and diluting them to a final concentration of 1 x 10^{-5} $molL^{-1}$.

2.3.2 Fluorescence Spectroscopy

In a typical fluorescence measurement, 2 ml BSA was added to quartz cell (1.0 x 1.0 cm). Fluorescence quenching spectra were recorded at 250-450 nm. The width of the excitation and emission slit was set to 15 and 4 nm respectively. The excitation wavelength of BSA was 285 nm. The BSA was titrated by successive additions of 2 x 10^{-6} $molL^{-1}$ metal complex solutions. Titrations were done manually by using micro-injector.

2.3.3 UV-Vis Spectroscopy

The absorption spectra of BSA and BSA-metal complex system were recorded in the range of 240-350 nm. The concentration of BSA and metal complex was 2 x 10^{-6} $molL^{-1}$.

2.3.4 Molecular docking studies

Molecular docking technique is useful in understanding the ligand-protein interactions which give additional support to our experimental results. The structures of the complexes were sketched by CHEMSKETCH and were converted from mol format to pdb format by OPENBABEL. The structure of BSA was obtained from protein data bank (pdb id: 3V03). The molecular docking studies were performed by using HEX 6.0 software. The docked poses were visualized by PyMOL.

RESULTS AND DISCUSSION

The ligand **L** was synthesized by the condensation of 9,10-Phenanthrenequinone and L-Tryptophan, and its complexes with Mn(III) and Fe(III) were also prepared **(scheme 1)**. The ligand is stable in air and soluble in common organic solvents like chloroform, ethanol and partially soluble in methanol. Its complexes are stable in air, and soluble in DMF & DMSO etc but insoluble in common organic solvents. Several attempts failed to obtain a single crystal suitable for X-ray crystallography. However, the analytical, spectroscopic and magnetic data enable us

to predict the possible structure of the synthesized complexes. All the synthesized compounds give satisfactory elementary analysis results.

3.1 Vibrational spectroscopy

The FT-IR spectra of ligand (L) and its metal complexes (MnL and FeL) are shown in supplementary file (Fig. S1, Fig. S2 & Fig. S3) respectively. The IR spectra of ligand (Fig. S1) shows an intense peak at 1673 cm^{-1} which is assigned to the imine (-C=N) stretching. The intense peak at 1590 cm^{-1} corresponds to (COO^-) asymmetric stretching and the peak at 1447 cm^{-1} is due to (COO^-) symmetric stretching vibration of carboxylic acid group. But in the IR spectra of complexes (Fig S2 and S3), the imino (C=N) stretching frequency has been shifted to lower frequency regions 1659 and 1663 cm^{-1} respectively, compared to that of the free ligand (1673 cm^{-1}). This indicates the coordination of imino nitrogens to the metal ions [19]. This is further supported by the presence of M-N bands (430 and 439 cm^{-1}). Moreover, the absorption band due to the asymmetric stretching vibrations of COO^- group has been shifted from 1583 to 1576 cm^{-1}, and the symmetrical stretching band is shifted from 1439 to 1402 cm^{-1}, which confirms the bonding of the metal ions by the carboxylato oxygen atom [20]. This is also confirmed by the formation of M-O bands at 530 and 531 cm^{-1} for MnL and FeL complexes respectively.

3.2 ^{13}C NMR spectra

The ^{13}C-NMR spectrum of the ligand (L) is shown in Fig S4. The signals obtained in the range 101.71-136.16 ppm are due to aromatic carbon atoms. The signal at 163.68 ppm corresponds to the azomethine carbons and the signal exhibited at 180.44 ppm is due to the carboxylate carbons.

3.3 Mass spectra

The EI mass spectrum (Fig S5) of ligand shows the molecular ion(M^+) peak at m/z =580 corresponding to the molecular weight of the ligand. The peaks at m/z = 550, 408, 376, 247, 230, 203, 175, 143, 125 and 71 corresponds to various fragments $C_{36}H_{26}N_4O_2$, $C_{26}H_{19}N_3O_2$, $C_{25}H_{18}N_3O$, $C_{16}H_{10}NO_2$, $C_{15}H_{11}N_2$, $C_{11}H_{10}N_2O_2$, $C_{14}H_8$, $C_{10}H_9N$, $C_5H_6N_2O_2$ and $C_2H_2NO_2$ respectively which confirms the structure of the ligand.

3.4 Electronic spectra, molar conductance and magnetic measurements

The electronic spectra of the complexes are given in Fig 1a and 1b. The UV-Vis spectrum of MnL comprises two absorption regions. On the basis of their energies and intensities, the band in the first region at 300 nm should be ligand field absorptions. The less intense and broad d-d bands in the second region around 580 nm and 730 nm correspond to $^5B_{1g} \rightarrow {}^5E_g$ and $^5B_{1g} \rightarrow {}^5B_{2g}$ transitions respectively. It confirms the tetragonally distorted octahedral geometry for the MnL complex [21]. The electronic spectra of FeL complex show two absorption bands at 700 nm and 300 nm. These bands can be assigned respectively to $^6A_{1g}(S) \rightarrow {}^4T_{1g}(G)$ and $^6A_{1g}(S) \rightarrow {}^4E_g$ transitions of the Fe(III) ion in the octahedral environment [22]. These are further confirmed by the magnetic moment values 4.94 BM and 5.76 BM [21] for MnL and FeL respectively suggesting the octahedral geometry.

The molar conductance values of MnL and FeL complexes in DMF are 51.35 and 51.95 suggesting the 1:1 electrolytic nature of the complexes [23].

3.5 EPR Spectral Studies

The solid state X-band EPR spectrum of the FeL complex in liquid nitrogen temperature (LNT) is illustrated in Fig 2. The spectrum shows six hyperfine lines, indicating the presence of five free electrons in the complex. This observation agrees well with magnetic moment value. The g_{av} value of 2.0 confirms the distorted octahedral geometry for the complex [24, 25].

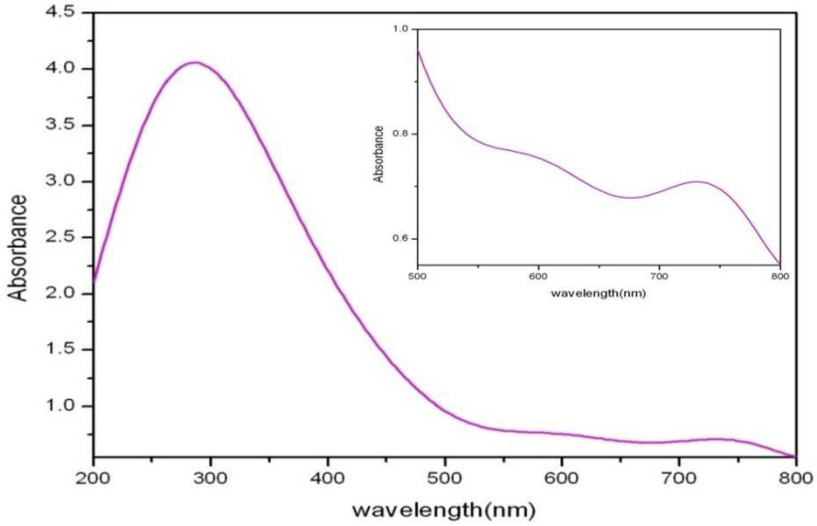

Fig 1a Electronic spectra of MnL complex

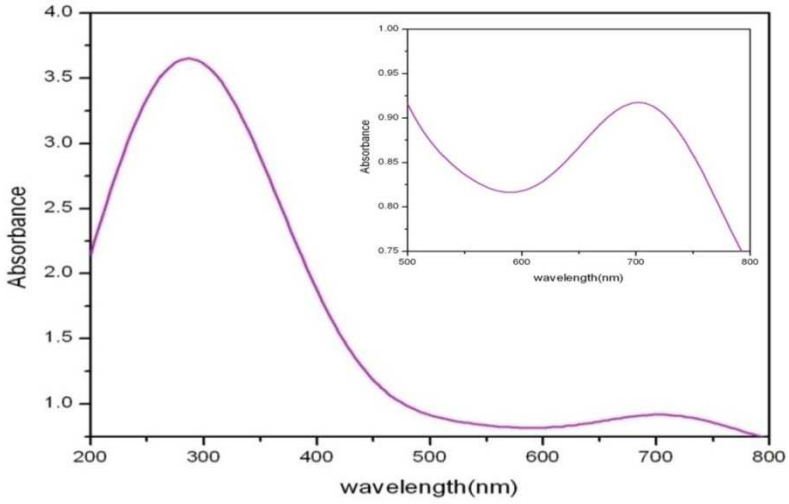

Fig 1b: Electronic spectra of FeL complex

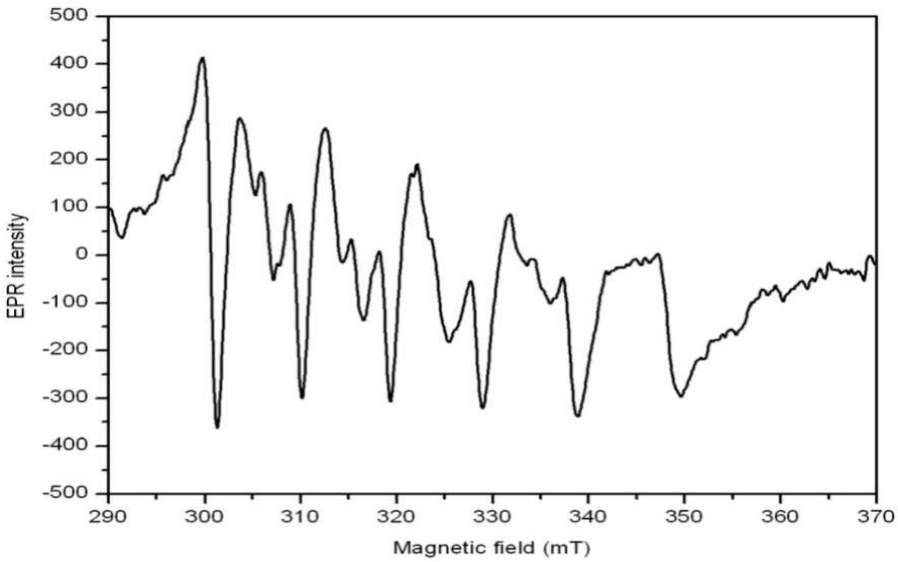

Fig 2: Solid state X-band EPR spectrum of FeL complex

3.6 Thermal studies

The thermograms of MnL and FeL complexes are illustrated in Fig 3a and 3b. The sample was heated at 1 atm pressure with a heating rate of 10 ^{0}C min^{-1} and a temperature range of 20–700 ^{0}C in air. The thermogram of the MnL exhibits decomposition between 250-300 ^{0}C with a weight loss of 5%. This is assigned to the removal of two coordinated water molecules. The sharp loss of weight of 83% between 375-425 ^{0}C corresponds to decomposition of organic moiety.

In FeL complex the decomposition between 250-300 ^{0}C with 5.5% weight loss is associated with the removal of two coordinated water molecules. The sharp loss of weight of 83% between 450-525 ^{0}C in the TGA curve represents the decomposition of organic moiety. Further horizontal constant curve in both the complexes may be due to the presence of metal oxides residue in the remaining part [26].

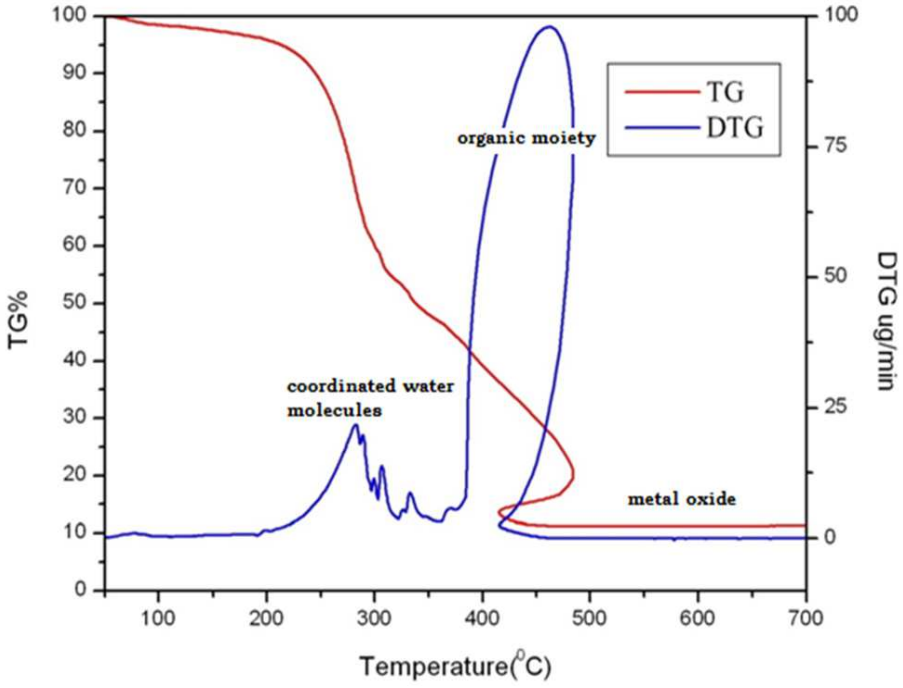

Fig 3a: TG/DTG curve of MnL

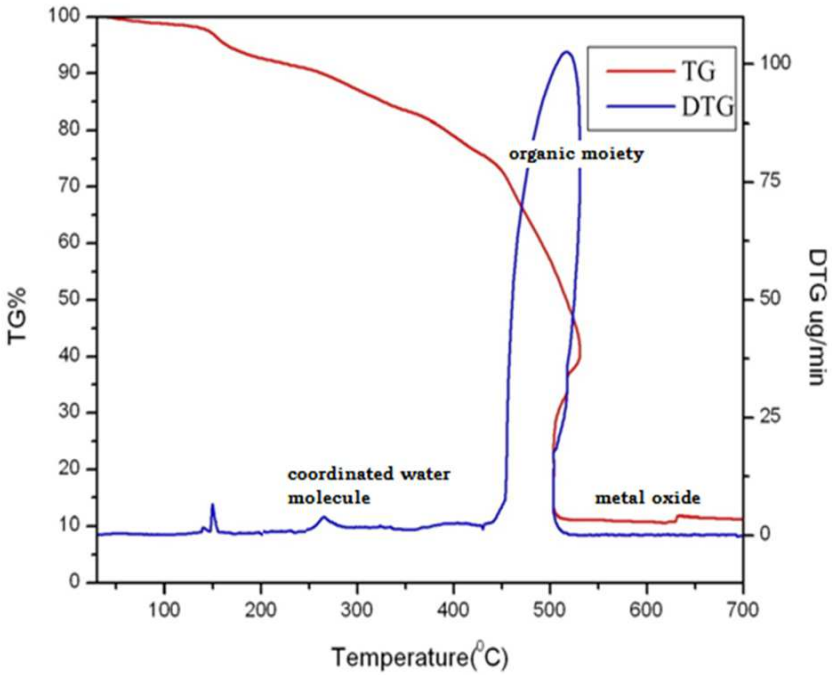

Fig 3b: TG/DTG curve of FeL

3.7 BSA binding studies

3.7.1 Fluorescence spectroscopy

On excitation of BSA at 285 nm, it emits fluorescence at 340 nm. The fluorescence behavior of BSA is due to the presence of three fluorescent amino acid residues i.e., tryptophan, tyrosine and phenylalanine. On the addition of metal complexes, the quenching of BSA fluorescence occurs.

The quenching of BSA fluorescence by metal complexes proceeds via dynamic/static quenching. Dynamic quenching arises due to diffusion and the formation of non-fluorescent ground-state complex leads to static quenching [27]. The fluorescence quenching is described by the Stern-Volmer relation [28].

$F_0/F = 1+ K_{sv}[Q] = 1+ K_q\tau_0[Q]$

Where, F_0 and F represent the fluorescence intensity in the absence and presence of quencher respectively. K_{sv} is a linear Stern-Volmer quenching constant, [Q] is the concentration of quencher, K_q is the quenching rate constant and τ_0 is the fluorescence lifetime of the protein in the absence of quencher. In the case of fluorescence quenching of BSA, a linear plot of F_0/F against [Q] was obtained and from the slope, K_{sv} was calculated. τ_0 is the average life-time of BSA and is found to be 10^{-8} s [29]. The apparent bimolecular quenching rate constant K_q which is equal to K_{sv}/τ_0 represents whether the quenching of BSA by complexes proceed through static or dynamic mechanisms [30].

The successive additions of different concentration of metal complex solutions to BSA could decrease its fluorescence intensity at 340 nm but the emission maximum was not shifted to shorter or longer wavelength. This is illustrated in Fig 4a and 4b. The addition of metal complexes could alter the fluorophore environment in BSA by interacting with it, but the local dielectric environment of BSA was not changed. The K_{sv} and K_q values calculated at different temperatures are given in Table 1.

The Stern-Volmer quenching constants K_{sv} were found to decrease with increase in temperature and the K_q values were found to be larger than 2.0 x 10^{10} $Lmol^{-1}s^{-1}$ reported [31] for the maximum diffusion quenching rate constant of various quenchers with biopolymers. This indicates that the quenching of BSA by the metal complexes is static and not dynamic quenching.

Table 1: K_{sv} and K_q values of MnL and FeL complexes

Complex	T(K)	K_{sv} (x 10^4 $Lmol^{-1}$)	K_q (x 10^{12} $Lmol^{-1}s^{-1}$)
MnL	298	5.62	5.62
	304	5.54	5.54
	310	5.38	5.38
FeL	298	6.79	6.79
	304	6.21	6.21
	310	5.94	5.94

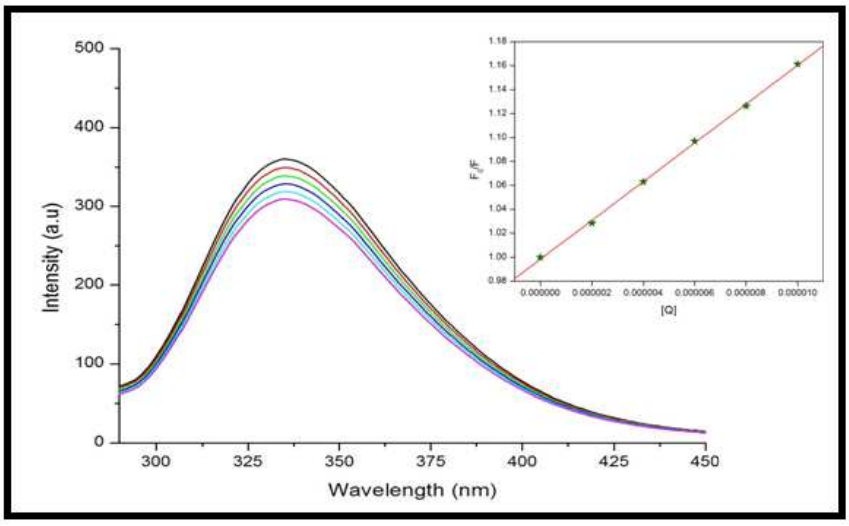

Fig 4a: Emission spectra of BSA in the presence of various concentration of MnL (T=298K), c(BSA)=2.0 x 10^{-6} $molL^{-1}$, c(MnL) = 2, 4, 6, 8, 10 x 10^{-6} $molL^{-1}$. Insert: Stern-Volmer plot for quenching of BSA by MnL

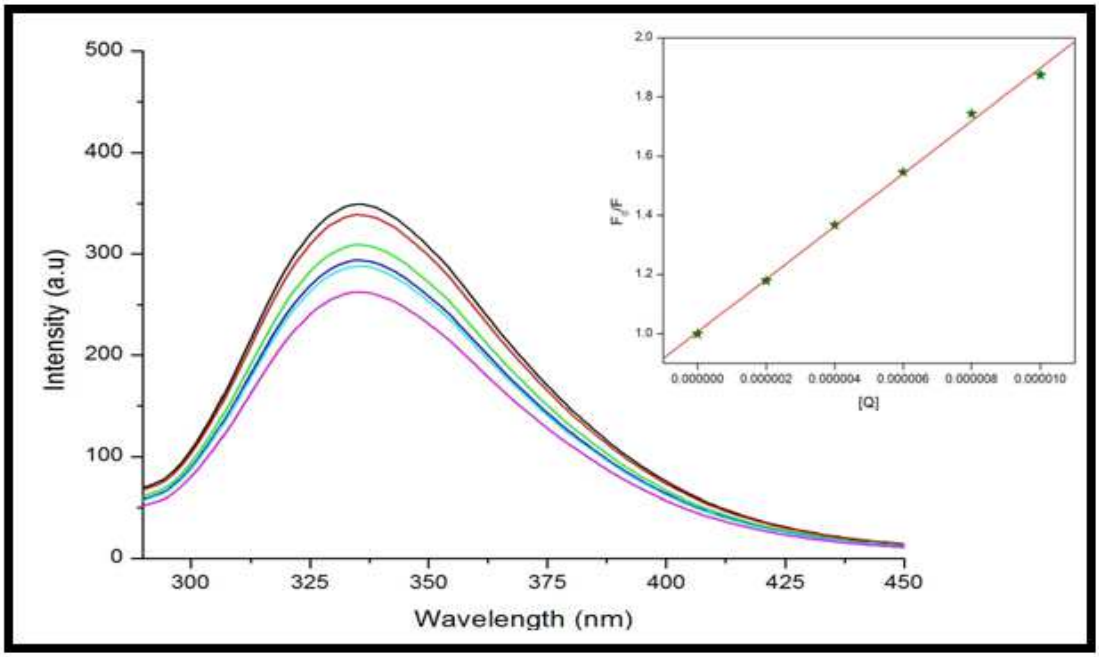

Fig 4b: Emission spectra of BSA in the presence of various concentration of FeL (T=298K), c(BSA)= 2.0 x 10^{-6} molL^{-1}, c(FeL) = 2, 4, 6, 8, 10 x 10^{-6} molL^{-1}. Insert: Stern-Volmer plot for quenching of BSA by FeL

3.7.2 Absorption spectroscopy

In order to confirm the quenching mechanism, the UV-Vis absorption spectra of BSA and metal complex solutions were also recorded. As shown in Fig 5a and 5b, the absorption intensity of BSA at 285 nm was slightly shifted to a longer wavelength upon addition of metal complex solutions. This confirms that the quenching mechanism of BSA by metal complexes arises as a result of static quenching i.e., due to complex formation between the molecules of BSA and metal complexes.

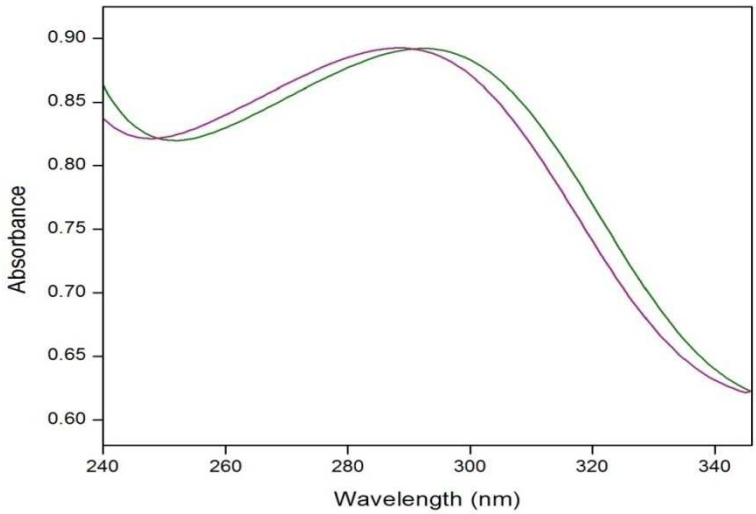

Fig 5a: UV-Vis absorption spectra of BSA and BSA-MnL solutions: c(BSA) = c(MnL) = 2 x 10^{-6} molL^{-1}

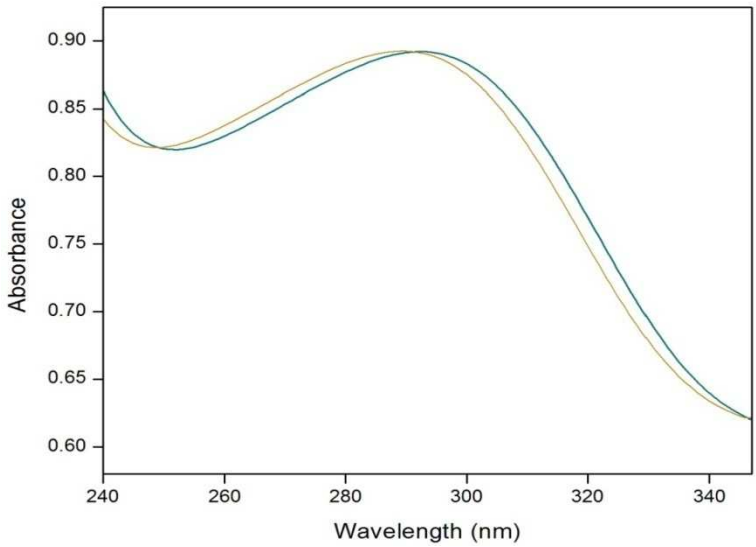

Fig 5b: UV-Vis absorption spectra of BSA and BSA-FeL solutions: c(BSA) = c(FeL) = 2 x 10^{-6} $molL^{-1}$

3.7.3 Analysis of binding constants, binding sites and binding energy

For static quenching, when the metal complexes bind to BSA, the binding constant (K_b) and the number of binding sites (n) can be obtained from the following equation [32],

$$\log\left(\frac{F_0 - F}{F}\right) = \log K_b + n \log[Q]$$

Where F_0 and F represent the fluorescence intensities in the absence and presence of quencher and [Q] is the concentration of the quencher. The values of K_b and n are obtained from the linear fitting plots of log [(F_0-F)/F] *vs.* log [Q] (Fig 6a. and 6b) which are furnished in Table 2. The results suggest that there exist a strong binding force between the BSA and the metal complexes. The hydrophobic metal complexes can interact with BSA by entering into the hydrophobic cavity present in it. The number of binding sites for both the complexes is approximated to 1 which suggests that the metal complexes can bind to protein through only one binding site.

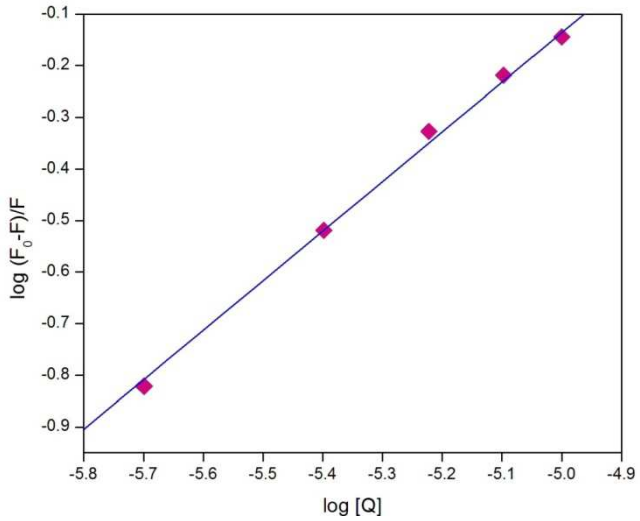

Fig 6a: Plot of log[(F_0-F)/F] *vs* log[Q] for BSA-MnL complex at 298 K

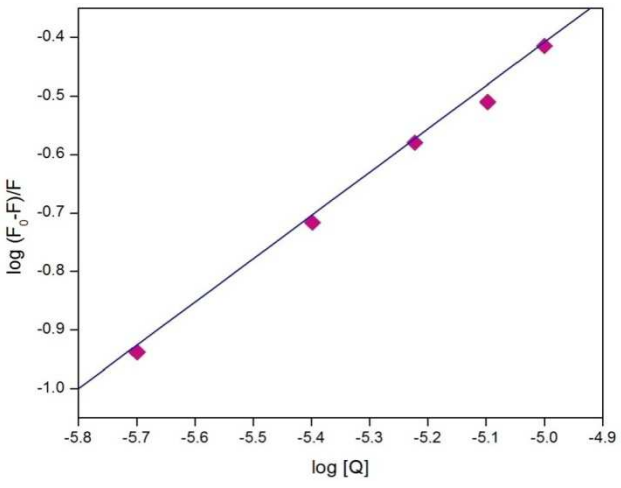

Fig 6b: Plot of log[(F_0-F)/F] *vs* log[Q] for BSA-FeL complex at 298 K

3.7.4 Thermodynamic parameters

The drug molecules interact with BSA through electrostatic interactions, hydrogen bonds, hydrophobic forces and Vander Waals interactions [33]. In order to make clear the interaction of the complexes with BSA, the thermodynamic parameters, Gibbs free energy changes (ΔG), enthalpy changes (ΔH) and entropy changes (ΔS) were calculated by Van't Hoff equation. The signs and magnitudes of the thermodynamic parameters (ΔH and ΔS) explains the type of forces involved in the binding process. Consequently, the binding constant at three different

temperatures i.e. 298 K, 304 K and 310 K were studied. At these temperatures the BSA would not undergo any structural degradation. The thermodynamic parameters were calculated from the Van't Hoff equation: [34]

$$\ln k = \frac{-\Delta H}{RT} + \frac{-\Delta S}{R}$$

$$\Delta G = -RT \ln K$$

$$\Delta S = \frac{\Delta H - \Delta G}{T}$$

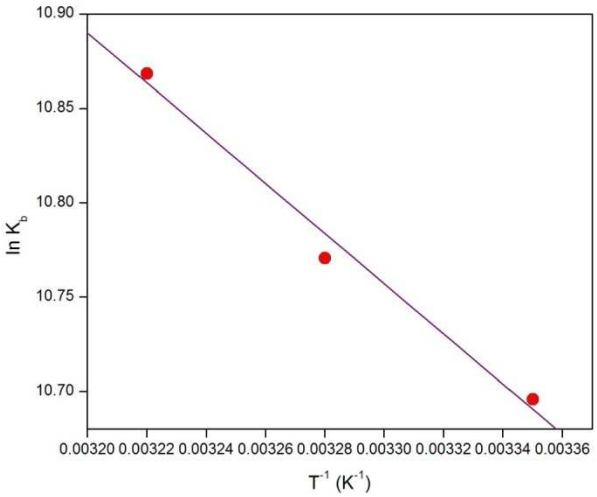

Fig 7a: Van't Hoff plot for the interaction of BSA with MnL complex

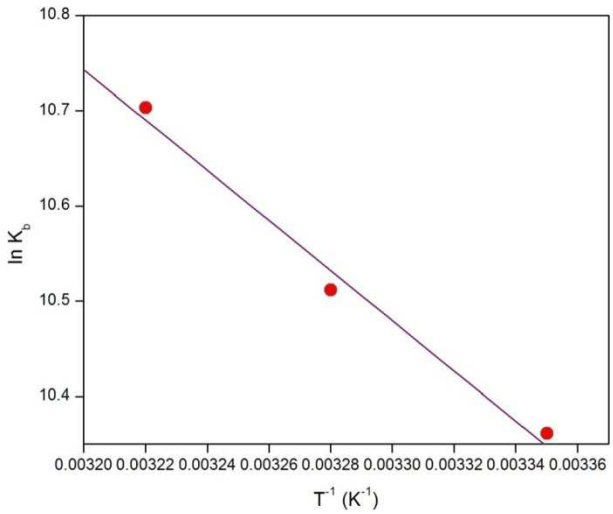

Fig 7b: Van't Hoff plot for the interaction of BSA with FeL complex

From the above equation it seems that there exists good linear relationship between lnK and 1/T. The ΔH and ΔS values are obtained from the slopes and ordinates at the origin of the fitted lines. (Fig 7a and 7b)

The positive enthalpy change (ΔH) and entropy change (ΔS) are linked with hydrophobic interactions. The negative values of ΔH and ΔS are associated with hydrogen bonding and Vander Waals interactions whereas the very low positive or negative ΔH and positive ΔS values are characterized by electrostatic interactions.

From the results obtained (Table 3) it is evident that the metal complexes are bound to BSA by electrostatic interactions and also the negative values of ΔG show the spontaneity of BSA-metal complex interaction.

Table 2: Binding constant(K_b) and Binding site(n) values of MnL and FeL complexes

Complex	T (K)	Binding constant (x 10^4 $Lmol^{-1}$)	Binding site
MnL	298	4.42	0.96
	304	4.76	1.04
	310	5.26	1.07
FeL	298	3.28	0.98
	304	3.36	0.99
	310	4.66	1.08

Table 3: Thermodynamic parameters of the binding interaction of metal complexes with BSA

Complex	T (K)	ΔH ($KJmol^{-1}$)	ΔS ($Jmol^{-1}K^{-1}$)	ΔG ($KJmol^{-1}$)
MnL	298	-13.30	15.148	-26.51
	304			-27.23
	310			-28.02
FeL	298	-26.36	19.178	-25.76
	304			-26.35
	310			-27.71

3.7.5 Energy transfer between the complexes and BSA

Fluorescence resonance energy transfer (FRET) depends on the distance between the molecules in their excited states. Generally, FRET occurs when the emission spectrum of a donor overlaps with the absorption spectrum of acceptor. The extent of energy transfer between the fluorophore and the drug molecule is determined from the extent of spectral overlap between emission spectrum of the donor and absorption spectra of the acceptor [35]. FRET is an

important method for to study a wide range of biological process [36]. From the Forster's theory, the efficiency of energy transfer, E is calculated as follows, [37]

$E = 1 - F/F_0 = R_0^6 / (R_0^6 + r^6)$

Where F_0 is the fluorescent intensity of BSA, F is the fluorescent intensity of BSA on addition of the metal complexes which is equal to the concentration of BSA, 'r' is the distance from the donor to the acceptor and R_0 is the Forster critical distance where the efficiency of energy transfer is 50%. R_0 can be calculated from donor emission and acceptor absorption spectra using the Forster formula, [38]

$R_0^6 = 8.8 \times 10^{-25} k^2 n^{-4} \Phi J$

K^2 is the orientation factor related to the geometry of the dipoles of the donor and acceptor and $k^2 = 2/3$ for random orientation as in fluid solution; n is the average refractive index of medium (n = 1.336 [39]); Φ is the fluorescence quantum yield of the donor and for BSA it is 0.15 [40]; J is the spectral overlap between the donor emission and the acceptor absorption and is calculated as follows: [41]

$$J = \frac{\Sigma\, \varepsilon(\lambda)\, F(\lambda)\, \lambda^4\, \Delta\lambda}{\Sigma\, F(\lambda)\, \Delta\lambda}$$

F(λ) is the corrected fluorescence intensity of the donor in the wavelength range λ, ε(λ) is the molar absorptivity of the acceptor at wavelength λ.

The overlap of the fluorescence emission spectrum of BSA and the absorption spectrum of MnL and FeL are shown in Fig 8a and 8b. The energy transfer parameters for the interaction of metal complexes with BSA are given in Table 4.

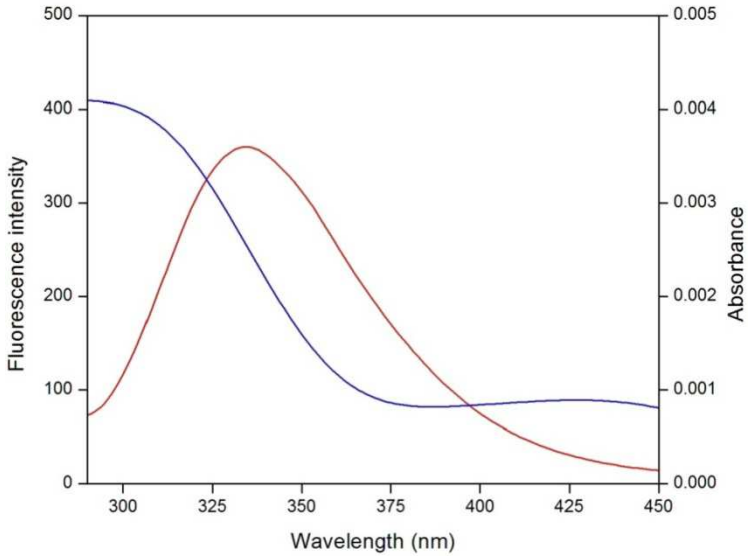

Fig 8a: Spectral overlap of UV-Vis absorption spectrum of MnL with the fluorescence emission spectrum of BSA. c(BSA) = c(MnL) = 2 x 10^{-6} molL^{-1}, T = 298 K

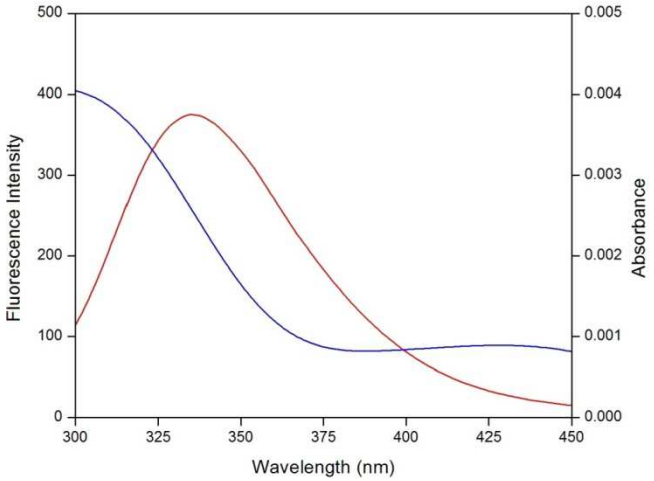

Fig 8b: Spectral overlap of UV-Vis absorption spectrum of FeL with the fluorescence emission spectrum of BSA. c(BSA) = c(FeL) = 2 x 10^{-6} molL^{-1}, T = 298 K

From the calculations, it was found that the distance (r) between the donor and acceptor is smaller than 8 nm [42], which indicates that there is high possibility for energy transfer from BSA to metal complexes.

Table 4: Energy transfer parameters for the interaction of metal complexes with BSA

complex	J (10^{-15} cm^{3}Lmol^{-1}	R_0 (nm)	E	r (nm)
MnL	2.27	1.91	0.11	2.70
FeL	3.79	2.08	0.17	2.71

3.7.6 Molecular docking studies

From the 3-D structure of crystalline albumin it was found that BSA is made up of three homologous domains (I, II and III); I (residues 1-183), II (residues 184-376) and III (residues 377-583), each containing two subdomains (A and B) forming a heart shaped molecule, which is separated into nine loops through 17 disulphide bonds, each one formed by six helices. The secondary structure of BSA is dominated by α-helix. It is suggested that the drug molecules could bind to BSA through hydrophobic cavities present in subdomains IIA and IIIA. The subdomain IIA contains the tryptophan residue 212 (Trp-212) [43]. The hydrophobic cavity present in subdomain IIA plays an important role in absorption, metabolism and transportation of BSA.

The minimum energy conformer showed that the complexes MnL and FeL bind within the hydrophobic pocket of sub-domain IIA as shown in Fig 9a and 9b for MnL and FeL complexes respectively.

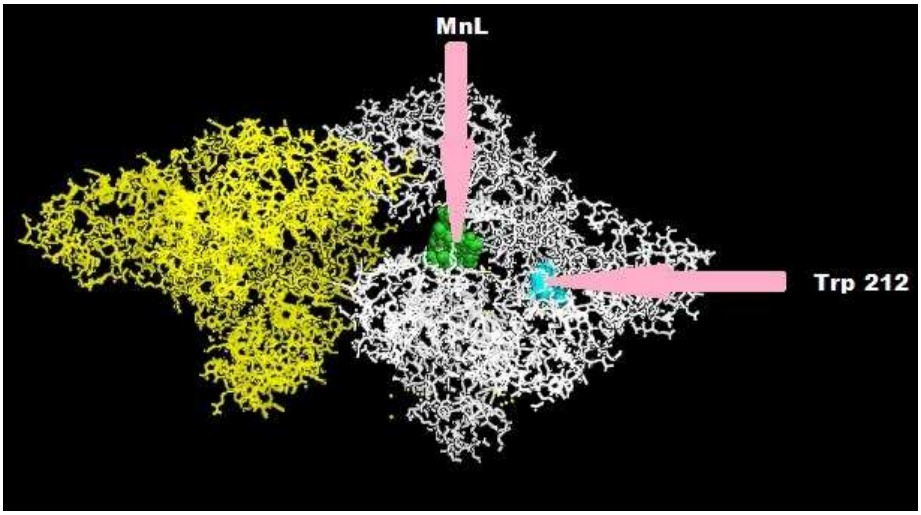

Fig 9a: Molecular docked model of MnL located within sub-domain IIA of BSA

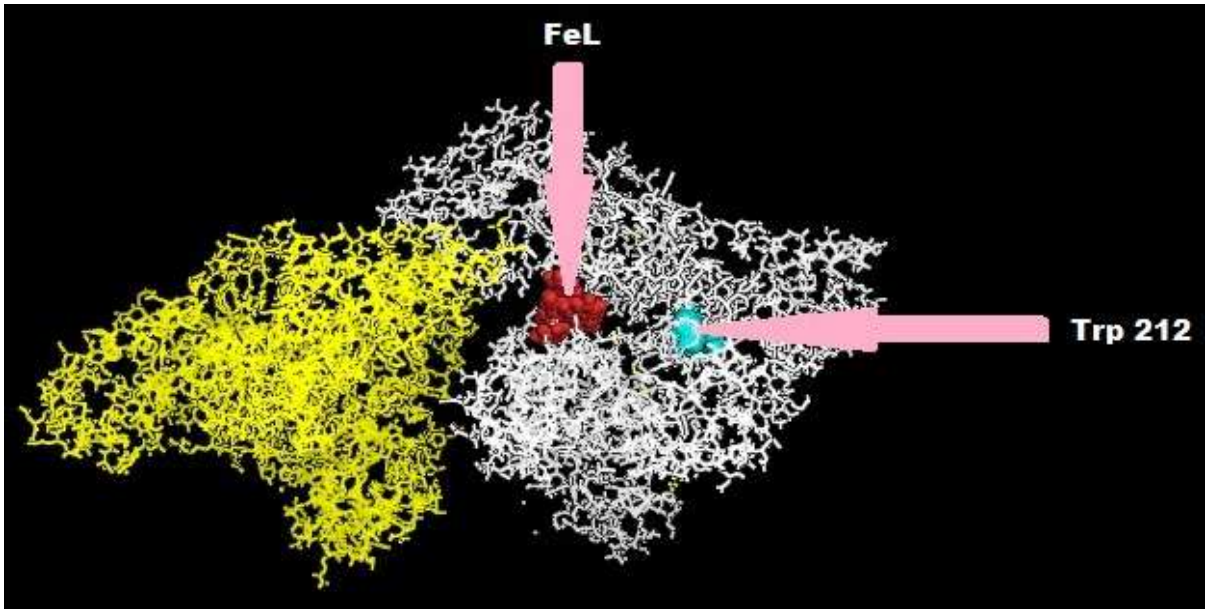

Fig 9b: Molecular docked model of FeL located within sub-domain IIA of BSA

CONCLUSION

In the present work a new tetradentate ligand and its Mn(III) and Fe(III) metal complexes were synthesized from 9,10-Phenanthrenequinone and L-tryptophan and characterized using various analytical and spectroscopic tools. The electrochemical and thermal studies were also carried out. The interaction of these metal complexes with BSA was studied using emission and absorption spectra. It was found that the metal complexes could quench the intrinsic fluorescence of BSA through static quenching. The enthalpy change and entropy change reveal that the metal complexes are bound to BSA by electrostatic interactions into the hydrophobic pocket of subdomain II A of BSA which is supported by the molecular docking studies. The distance between the BSA and MnL & FeL was found to be 2.70 and 2.71 respectively which indicates that the energy transfer occurs with high possibility.

REFERENCES

[1] P. A Vigato, S. Tamburini, *Coord. Chem. Rev*., **2004**, 248, 1717-2128.
[2] K. Palme, F. Nagy, *Cell*., **2008**, 133, 31-32.
[3] D. C. Carter, J. X. Ho, *Adv. Protein. Chem*., **1994**, 45, 153-203.
[4] W. E. Klopfenstein, *Biochem. Biophys. Acta*, **1969**, 181, 323.
[5] W. G. Unger, *J. Pharm. Pharmacol*., **1972,** 24, 470-477.
[6] A. Schrepartez, B. Cuenoud, *J. Am. Chem. Soc*., **1990**, 112, 3247.
[7] C. C. Cheng, S. E. Rokita, c. Burrows, *Angew. Chem*., **1993,** 105, 290.
[8] U. K. Hansen, *Pharmacol. Rev*.. **1981,** 33, 17-53.
[9] G. Zhang, Q. Que, J. Pan, J. Guo, *J. Mol. Struct*., **2008,** 881, 132-138.
[10] W. Y. He, Y. Li, C. X. Xue, Z. D. Hu, X. G. Chen, F. L. Sheng, *Bioorgan. Med. Chem*., **2005**, 13, 1837-1845.
[11] F. Y. Wu, Z. J. Ji, Y. M. Wu, X. F. wan, *Chem. Phys. Lett*., **2006,** 424, 387-393.
[12] B. K. Jin, L. P. Lu, *Chin. Chem. Lett*., **2001,** 12, 989.
[13] H. Y. Shrivastava, M. Kanthimathi, B. U. Nair, *Biochem. Biophys. Res. Commun*., **1999,** 265, 311.
[14] S. J. Lau, T. P. A. Kruck, b. Sarkar, *J. Biol. Chem*., **1974,** 249, 5878.
[15] C. Tanford, *J. Am. Chem. Soc*., **1952,** 74, 211.
[16] H. A. Saroof, H. J. Mark, *J. Am. Chem. Soc*., **1953**, 75, 1420.
[17] M. C. Beinfield, D. A. Bryce, D. Kochavy, A. Martonosi, *J. Biol. Chem*., **1975,** 250, 6282.
[18] E. Alarcon, A. Aspee, M. Gonzalez-Bejar, A.M. Edwards, E. Lissi, J.C. Scaiano, *Photochem. Photobiol. Sci*., **2010**, 9, 861-869.
[19] J. R. Ferraro, "*Low frequency Vibrations of Inorganic and Coordination Compounds*", 3rd Edn, Wiley Interscience, New York, **1978**.
[20] S. Theodore David, R. Antony, K. Saravanan, K. Karuppasamy, S. Balakumar, *Spectrochim. Acta A*, **2013,** 103, 423–430.
[21] T.S. Davis, J. P. Fackler, M. J. Weeks, *Inorg Chem*., **1968**, 7, 1994.

[22] R. Sarika Yaul, R. Amit Yaul, B. Gaurau Pethe, S. Anand Aswar, *American-Eurasian Journal of scientific research*, **2009,** 4, 229-234.
[23] W. J. Geary, *Coord. Chem. Rev*., **1971,** 7**,** 81-122.
[24] J. E. Wertz, J. R. Bolton, Electron spin resonance, "*Elementary Theory and Practical Applications*", McGraw-Hill, USA, **1972**.
[25] Estevan V. Spinace, Dilson Cardoso, Ulf Schuchardt, *Zeolites*, **1997,** 19, 6-12.
[26] Lucie Trnkova, Iva Bousova, Vladimir Kubicek, Jaroslav Drsata, *Nat. Sci*., **2010**, 2, 563-570.
[27] Yanling Xiang, Fangying Wu, *Spectrochim. Acta A,* **2010,** 77, 430-436.
[28] O. Stern, M. Volmer, *Z. Phys*., **1919,** 20, 183-188.
[29] Bi, S., Y. Sun, C. Qiao, H. Zhang, C. Liu, J. Lumin., **2009,** 129, 541-547.
[30] Kaboudin, B., K. Moradi, M. Faghihi, F., Mohammadi, J. Lumin., **2013,** 139, 104-112.
[31] H. Cao, D. Wu, H. Wang, M. Xu, *Spectrochim. Acta A*, **2009,** 73, 972-975.
[32] J. H. Yu, B. Li, P. Dai, S. G. Ge, *Spectrochim. Acta A*, **2009,** 74, 277-281.
[33] D. Leckband, *Annu. Rev. Biophys. Biomol. Struct*., **2000**, 29, 1-26.
[34] Zhang, Y.-Z., B. Zhou, X.-P. Zhang, P. Huang, C.-H. Li, Y. Liu , J. Hazard. Mater., **2009,** 163, 1345-1352.
[35] Q. Zho, J. Xiang, Y. Tang, J. Liao, C. Yu, H. Du, Q. Yang, G. Xu, Pestic. *Biochem. Physiol*., **2008**, 92, 43.
[36] M. Gharagozlou, D. M. Boghaei, *Spectrochim. Acta A*, **2008,** 71, 1617.
[37] T. Forster, *Ann. Phys*., **1948,** 2, 55-75.
[38] A. Mahammed, H. B. Gray, J. J. Weaver, K. Sorasaenee, Z. Gross, *Bioconjugate Chem*., **2004,** 15, 738-746.
[39] N. Shaklai, J. Yguerabide, H. M. Ranney, *Biochemistry*, **1977**, 16, 5585.
[40] L. Cyril, J. K. Earl, W. M. Sperry, Biochemists' Handbook, E. & F. N. Spon, London, **1961**, p. 83.
[41] Yu, X., R. Liu, D. Ji, J. Xie, F. Yang, X. Li, H. Huang, P. Yi, Spectrochim. Acta A, **2010,** 77, 213-218.
[42] D. J. Li, J. F. Zhu, J. Jin, X. J. Yao, *J. Mol. Struct*., **2007,** 846, 34-41.
[43] B. Bhattacharya, S. Nakka, L. Guruprasad, A. Samanta, *J. Phys. Chem. B*, **2009,** 113, 2143-2150.